M. BRŮNA[1*], M. GALČÍK[1], A. SLÁDEK[1], D. MARTINEC[1]

POSSIBILITIES OF BIFILM AMOUNT REDUCTION IN Al CASTINGS BY GATING SYSTEM DESIGN OPTIMIZATION

Submitted work deals with the possibilities of reducing reoxidation by improved gating system design. The result of the reoxidation is the of furled oxide layers – bifilms. During experimental works, non-pressurized and naturally pressurized gating systems designs were introduced and evaluated. Mechanical properties, fracture area, hot tearing index, bifilm index and EDX analysis were used during evaluation. Paper aim is also to clarify the reoxidation phenomenon by visualization with the aid of ProCAST numerical simulation software. Achieved results clearly confirmed the positive effect of the naturally pressurized gating system, main emphasis needs to focus on finding the proper way to reduce the melt velocity. By using vortex element extension at the end of the runner was achieved positive results in term of reoxidation suppression.

Keywords: reoxidation, bifilm, gating system, aluminium alloys, mechanical properties

1. Introduction

Importance of aluminium cast alloys and their use in recent years reflects the demand for light-weight construction with maintaining good mechanical properties. Aluminium alloys castings have been rarely used in the safety-critical application despite of many positive characters. The reason is the high variability of mechanical properties (even if there is an effort to maintain identical production conditions). In 1987 Svoboda [1] made research from 14 independent foundries on 500 castings. The result showed that 84% of foundry defects are caused by reoxidation. There is no similar research recently and although it was focused on the steel castings, the impact of even larger extent can be expected for aluminum alloys.

Reoxidation processes arise because of melt critical velocity associated with extent turbulence causing bifilm formation. Bifilms are basically surface oxide layers connected dry side to dry side by the effect of immersion and transport through the bulk of the metal (Fig. 1) [2,3].

Campbell [4] as the first defined the term "bifilms" and pointed out their negative potential affecting casting properties. Bifilms are very small and have compact shape, so they can penetrate through all the filling system and ends in the solidifying casting. It was also pointed out, that after entrainment due to internal turbulence, the bifilm become convoluted and in this compact form he can easily transport through entire gating system. One of the possibilities how to easily suppress the negative influence of reoxidation is by fundamental change of approach to the gating system design [5].

Fig. 1. Scheme of the bifilm origin

[1] UNIVERSITY OF ŽILINA, FACULTY OF MECHANICAL ENGINEERING, DEPARTMENT OF TECHNOLOGICAL ENGINEERING, UNIVERZITNÁ 8215/1, 010 26 ŽILINA, SLOVAKIA

* Corresponding author: marek.bruna@fstroj.uniza.sk

2. Experimental materials and methods

Chemical composition of used alloy is shown in Table 1.

Chemical composition of AlSi7Mg0.3

Element	Si	Fe	Cu	Mn	Mg	Zn	Ti	Al
[wt. %]	7.3	0.15	0.03	0.10	0.3	0.07	0.15	bal.

Construction of the gating system is commonly divided into pressurized and non-pressurized gating systems, based on the so-called 'choke area'. These constructions designs are not sufficient in terms of suppressing the reoxidation. Therefore, it was necessary to design a different type of gating system – naturally pressurized. The system is designed without the 'choke area' as close as possible to 1:1:1 ratio, so that the melt is in all places in direct contact with the mold walls (except for the head area of flow) by natural backpressure in gating system due to friction resistance. Such a design is preferable because of the area exposed to further reoxidation is significantly smaller and it promotes the natural melt flow. Although this concept has been known for a long time, its use in practice is rare. Considered value of critical velocity in which turbulences occurs is 0.5 m.s^{-1}. To reduce melt velocity in naturally pressurized systems, the filters, various extensions of the runner or so-called vortex elements were used in previous research works [6-8]. The first part of the analysis focuses on the numerical simulation by ProCAST. Four types of gating systems were designed (Fig. 2). Two systems are common concepts of the non-pressurized gating system, where one have a slight modification of the runner (Fig. 2b). Following two systems are based on the concept of the naturally pressurized gating system (Fig. 2c), where one includes the modification of the runner as shown at Fig. 2d.

For the purposes of experiments, two types of castings were used. First casting design was intended for mechanical properties evaluation, second casting is designed to evaluate hot tear index, dimensions are shown at Fig. 3a,b.

By the numerical simulations, analysis of oxides and melt velocity during molds filling were evaluated. Subsequently, real casts were produced to be able to compare real results with the simulations. Casts were poured by gravity sand casting method (green sand). The melt temperature was 720 ± 5°C poured to a mold with temperature 20°C. The primary AlSi7Mg0.3 alloy was used without any modification. Three sets of the casts from every mold design concept were made.

3. Gating system calculation

Non-pressurized gating system

When calculating the gating system, the area of all cross-sections is decisive. The ratio of the cross-sectional areas in the gating system in the case of a unpressurized system gradually increases. Selected ratio was 1: 4: 4. The length between the
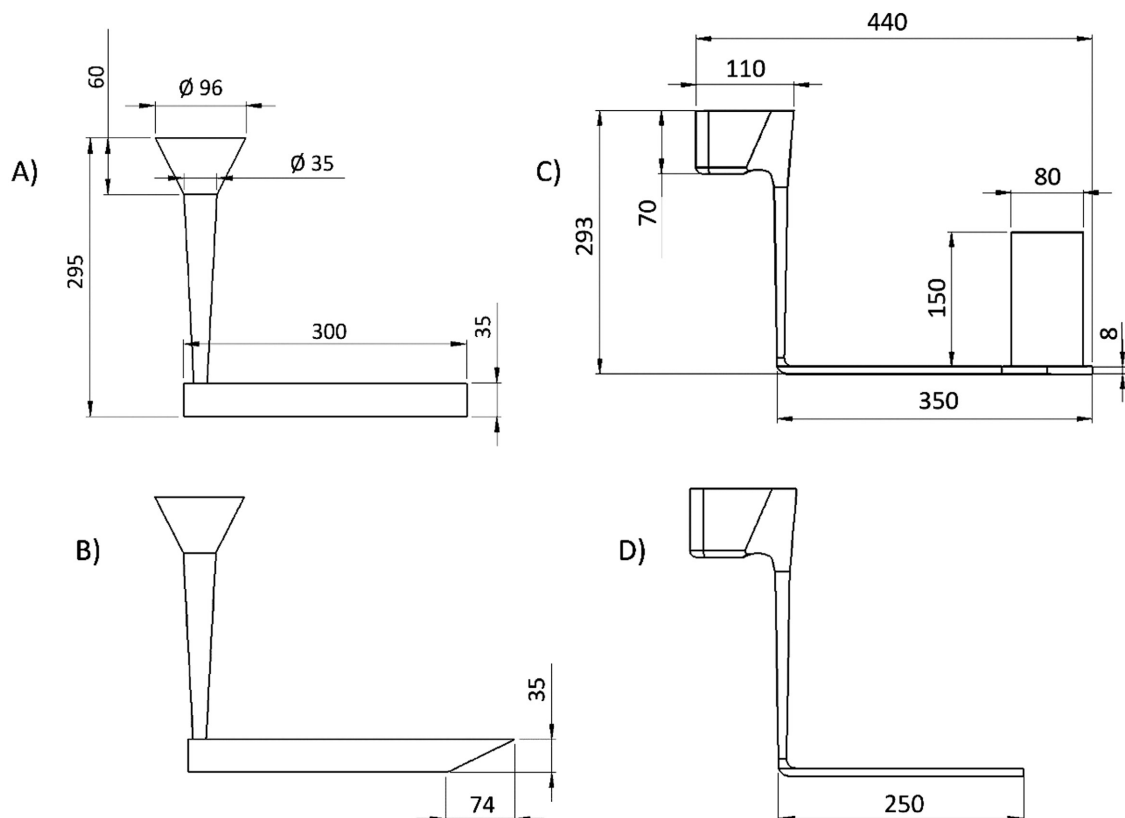

Fig. 2. Gating system design for experimental work a) non-pressurized gating system, b) non-pressurized gating system with modification of the runner, c) naturally pressurized gating system, d) naturally pressurized gating system with vortex extension
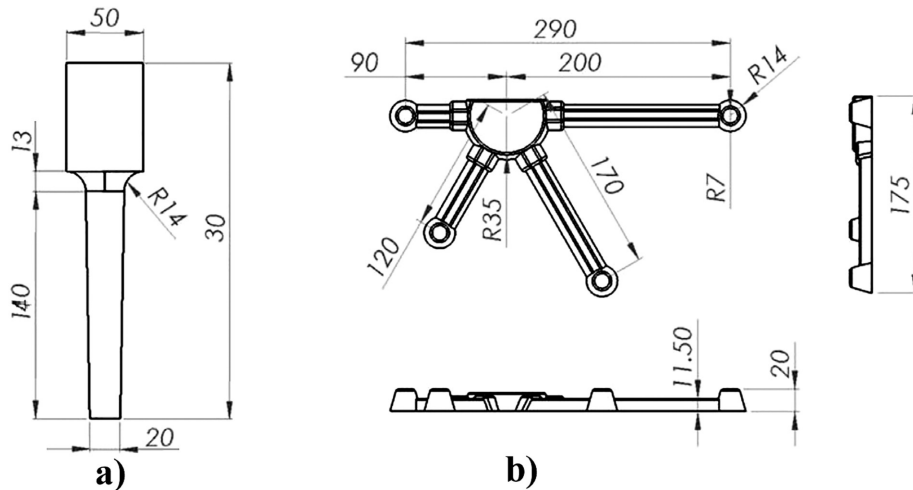
Fig. 3. Castings design a) Mechanical properties b) Hot tear index

runner and the first gate should be at least 120 mm. The choke area, from which is possible to calculate the values of other cross-sections according to the ratios is determined by the Eq. (1).

$$S_z = \frac{m_o}{\mu.\tau_L.\rho\sqrt{2.g.H_{str}}} \ [\text{mm}^2] \tag{1}$$

where m_0 is gross weight of casting [kg], H_{str} – mean metallostatic height [m], τ_L – pouring time [s], μ – coefficient of hydraulic resistance.

The pouring time is an important value, which, however, depends on many factors. As there is no general rule for determining its optimal value, it is determined according to the empirical relationships of many authors. In our case, due to the initial parameters, we choose the calculation of the optimal casting time according to Eq. (2).

$$\tau = 2,20\sqrt{0,4} = 1,4\,s \tag{2}$$

where s is the factor depends on the wall thickness of the casting and the type of material being cast ($s = 2,20$), m – weight of casting [kg]. The mean metallostatic height is determined according to the position of gates by the equation, Eq. (3).

$$H_{str} = 0,2 - \frac{0,1^2}{2x0,1} = 0,2 - 0,075 = 0,125\,\text{m} \tag{3}$$

Where H is initial maximum metallostatic pressure [Pa], P height of the casting above the level of the gates [m], C – total casting height [m]. After calculation of the required parameters, the determining cross section will be, Eq. (4).

$$S_z = \frac{0,4}{0,8.1,4.2500\sqrt{2.9,81.0,125}} = 101\,\text{mm}^2 \tag{4}$$

Since the sprue is cylindrical, we can determine the control section radius, Eq. (5).

$$S_k = \pi.r^2 \rightarrow r = \sqrt{\frac{S_k}{\pi}} = \sqrt{\frac{101}{3,14}} \cong 6\,\text{mm} \tag{5}$$

The area of the runner and gates will therefore be $S = 404$ mm^2. Calculation of gates will be performed only in the case of the castings intended for hot tear susceptibility. The cross-sections of the runner channel and the gates were chosen to be rectangular in shape with a different nominal value. For the rectangular cross-section of the runner is chosen the height value $b = 25$ mm, from which is calculated its length a, Eq. (6).

$$S = a.b \rightarrow a = \frac{S}{b} = \frac{404}{25} \cong 16\,\text{mm} \tag{6}$$

For the rectangular cross-section of the gates is chosen the height value b = 13 mm, from which is calculated the value of the length of the gates a, Eq. (7).

$$S = a.b \rightarrow a = \frac{S}{b} = \frac{404}{13} \cong 31\,\text{mm} \tag{7}$$

Naturally pressurized gating system

The naturally pressurized inlet system is characterized by the elimination of the choke areas and other elements that affect the natural progression of the melt. As the transitions of the individual parts of the inlet system are smooth and without a significant change in the shape of the individual cross-sections, the implementation of the calculation of such a system in the selected ratio 1: 1: 1 will be calculated. Regarding the casting time, Campbell [2] recommend to set its value at least twice as calculated value (the faster the filling, the more turbulent it will be). Since the values of the input quantities are the same with the previous system, the pouring time is set to $\tau_L \cong 3$ s. After determining the pouring time, the average and actual pouring rates are calculated. The average pouring rate is the ratio of the total weight of the cast metal for the total casting time, Eq. (8).

$$\text{Averange pouring rate} = \frac{m}{\tau_L} = \frac{1,4}{3} \cong 0,5\,\text{kg.s}^{-1} \tag{8}$$

The value of the actual casting rate is higher than the value of the average rate because the initial velocity at which the melt enters the system is not maintained. The speed of the metal decreases due to the filling of the mold, and if the level of metal in

the mold rises to the same height as the pouring cup, it reaches zero. To take this effect into account, it is appropriate to assume that the value of the actual pouring rate is approximately twice the value of the average rate, Eq. (9).

Actual pouring rate =

$$= 2x \text{ Average pouring rate} = 2.0,5 = 1\,\text{kg.s}^{-1} \quad (9)$$

Assuming that the metal is poured using a plug in the pouring cup, its initial velocity after removal of the plug will be zero and will gradually increase with the height value h through which it advances. The speed at which the melt will move at the point of entry of the melt into the sprue is determined by Eq. (10), where h_1 is depth of pouring cup = 50 mm.

$$v_1 = \sqrt{2.g.h_1} = \sqrt{2.9,81.0,05} \cong 0,7\,\text{m.s}^{-1} \quad (10)$$

The velocity at which the melt will move in the lower part of the sprue before it passes into the runner is determined analogously by Eq. (11).

$$v_2 = \sqrt{2.g.h_2} = \sqrt{2.9,81.0,225} \cong 2,12\,\text{m.s}^{-1} \quad (11)$$

Where: h_2 – height from the bottom of the pouring cup to the bottom of the sprue = 0,225 mm. It should be noted that a low velocity v_1 is associated with a larger cross-sectional area A_1 and at the bottom a higher velocity metal v_2 is associated with a smaller area A_2. Under this assumption, the falling melt is continuous and the stable flow is maintained by Eq. (12).

$$Q = v_1.A_1 = v_2.A_2 \quad (12)$$

In order to determine the cross-sectional areas of naturally pressurized gating system, it is necessary to know the value of the flow volume, which is calculated as a proportion of the actual pouring rate relative to the total cast weight and density of the aluminum alloy, Eq. (13).

$$Q = \frac{1,4\,\text{kg.s}^{-1}}{2500\,\text{kg.m}^{-3}} = 0,56\,\text{m}^3.\text{s}^{-1} \quad (13)$$

Since we know the values of all the necessary quantities, we can determine the cross-sections A_1 after modifying the equation Eq. (14):

$$Q = v_1.A_1 \rightarrow A_1 = \frac{Q}{v_1} = \frac{0,56}{0,7} \cong 800\,\text{mm}^2 \quad (14)$$

and A_2 by Eq. (15).

$$Q = v_2.A_2 \rightarrow A_2 = \frac{Q}{v_2} = \frac{0,56}{2,12} \cong 264\,\text{mm}^2 \quad (15)$$

For the rectangular upper cross-section of the sprue and thus the place of transition of the pouring cup into the sprue, we choose the value of the height $b_1 = 14$ mm, from which we calculate its length a_1, Eq. (16).

$$A_1 = a_1.b_1 \rightarrow a_1 = \frac{A_1}{b_1} = \frac{800}{14} \cong 55\,\text{mm} \quad (16)$$

Analogously, can be calculated the value of the length a_2 of the lower rectangular cross-section of the sprue, which is situated before the rounded transition to the runner, and for which the value of its height $b_2 = 8$ mm was chosen, Eq. (17).

$$A_2 = a_2.b_2 \rightarrow a_2 = \frac{A_1}{b_1} = \frac{264}{14} \cong 35\,\text{mm} \quad (17)$$

From the above calculations, the geometric parameters of the cross-sections of the sprue $A_1 = 14 \times 55$ mm and $A_2 = 8 \times 35$ mm were determined.

Since the surface ratios do not change, to simplify the process and at the same time maintain the continuity of flow, cross-sections of the runner, as well as the gates will be 8×35 mm.

4. Results of numerical simulation

Analysis of turbulence energy

The tracing indicator for turbulence energy was set to [100 cm^2.s^{-2}]. Based on the numerical simulation results (Fig. 4), the hypothesis that a non-pressurized gating system is insufficient in terms of reoxidation processes can be confirmed.

As a consequence of imperfectly filled runner, a large area of surface layer is exposed to oxidation, also breaking waves and bounce wave can occur at the end of the runner. The result of the first variant (Fig. 4a) shown that the melt suddenly bounce back, and the two surfaces are subsequently folded and joined, creating a large amount of bifilms. In the variant with modification in form of the gradual narrowing of the runner (Fig. 4b), there was a slight suppression of bouncing wave, but the area exposed to further oxidation remains extensive. In the case of a naturally pressurized gating system (Fig. 4c), the place for turbulence is eliminated by a completely filled space in every point of the system. The critical place of this concept is the gate area because of the melt high velocity without any slowing mechanism, which will be analyzed further. The best result was achieved in the naturally pressurized gating system with vortex extension of the runner (Fig. 4d). The melt flow was directed to a vortex element, which ensures calm continuity of flow in the runner. Turbulent energy is situated in the vortex element and other parts of the filling system are protected from the negative influence of reoxidation.

Analysis of the melt velocity

The velocity of the melt flow affects the character and scale of turbulence present during the gating system filling. The result of the melt flow rate analysis [m.s^{-1}] for the non-pressurized gating system, showed a reduction of the melt velocity in the choke area (Fig. 5a,b), which ensures calm filling in the gate area. However, the critical area of further reoxidation and the presence of the bouncing wave in the runner remains problematic.

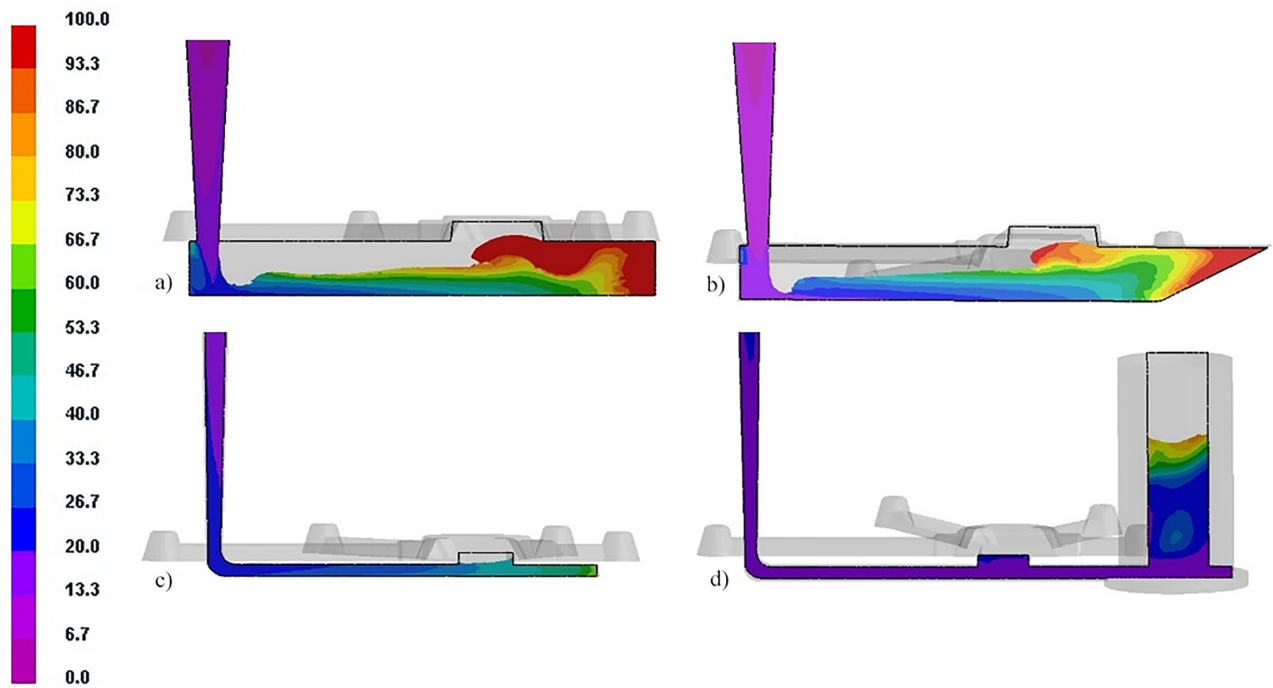553

Turbulent energy
[cm²/s²]

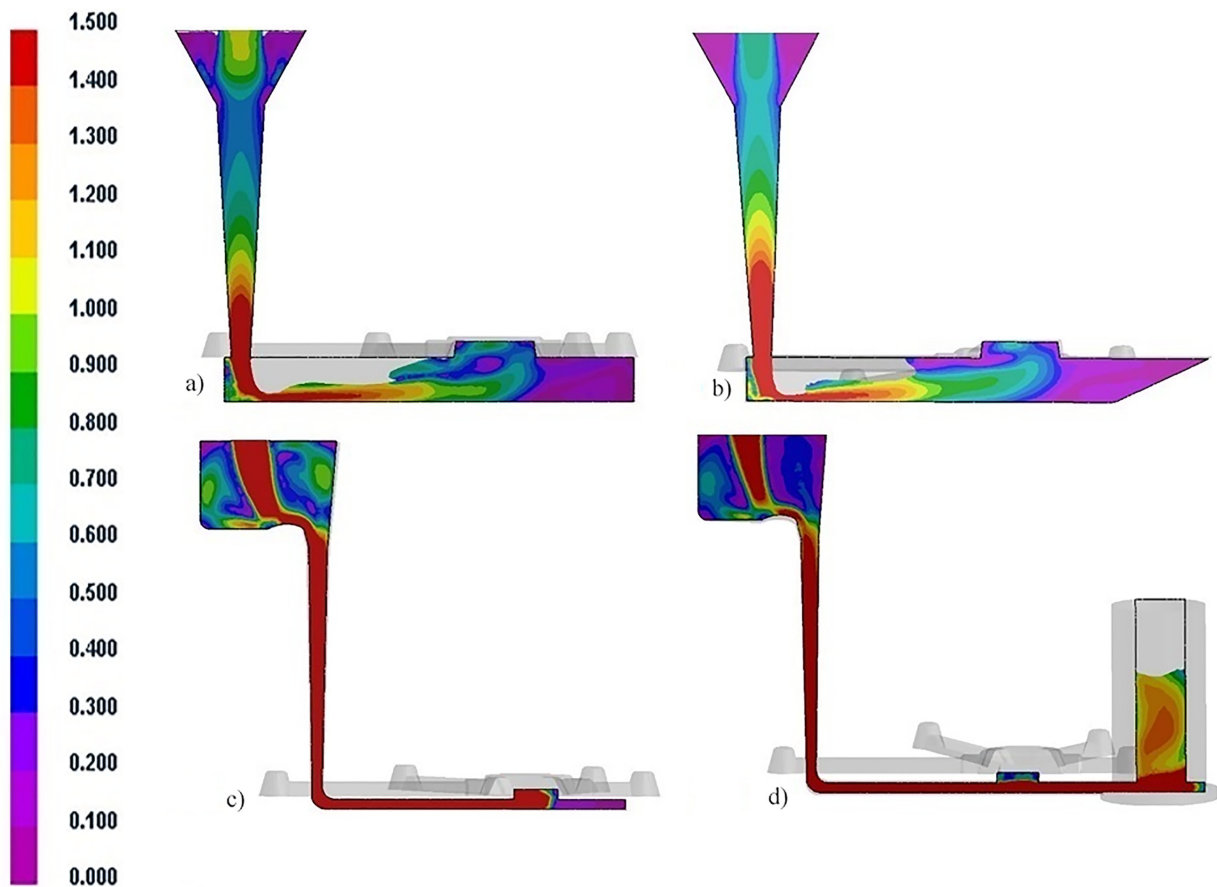Fig. 4. Result of the turbulence energy analysis

Velocity
[m/s]

Fig. 5. Analysis of the melt flow velocity

As mentioned before, in the naturally pressurized gating system is the critical velocity of the melt exceeded due to the absence of a mechanism to reduce it. Velocity energy at the end of the runner is transferred to the gate area (Fig. 5c), where the splashes occurs, resulting in the extensive reoxidation. At this point, all benefits of a perfectly filled gating system during the filling are lost. Numerical simulations have shown the best results as the concept of naturally pressurized gating system with runner modification (Fig. 5d). The energy of the melt flow is situated in the vortex element, which ensures a significant reduction of the melt velocity in the runner and also avoiding the splashes formation at the point of entry to the cast part of mold cavity. To better illustrate the described phenomenon occurring in the naturally pressurized gating system, melt spatter is shown on the casting design for the mechanical properties evaluation (Fig. 6).

Analysis of oxides occurrence

Entrained oxides are the result of the reoxidation processes and the final oxides amount in the casting depends on the flow velocity and the turbulence occurrence. Due to the imperfectly filled runner supporting the formation of reoxidation processes, the oxide occurrence is largely observed in the designs of the non-pressurized gating system (Fig. 7a,b). A lot of oxides oc-curs mainly in the ends castings of the system due to extensive turbulences at the end of the runner. The tracking indicator for oxide occurrence was set to value [0.5 cm^2.s].

In the case of the naturally pressurized gating system, splashes occur at the gate entry as a result of the above-mentioned high critical velocity, resulting in an increased content of oxides in all three castings (Fig. 7c). With the application of the vortex element, front head of the melt is concentrated to the cylindrical end, where is the flow directed to a tangential gradient eddying motion and the oxides are trapped in this area (Fig. 7d). There is achieved a significant reduction in the melt velocity, which then enters through the gate at lower speed avoiding spattering and ensure the calmer filling.

5. Experimental casts

Evaluation of mechanical properties and hot tearing index

The tensile strength is affected by the number of bifilms that may be present in the casts. The higher amount of bifilms, the sooner the material fraction can occur. The results showed that the higher tensile strength was obtained by using the naturally pressurized gating system with vortex extension of the runner. Results for tensile strength and elongation are presented in Fig. 8.
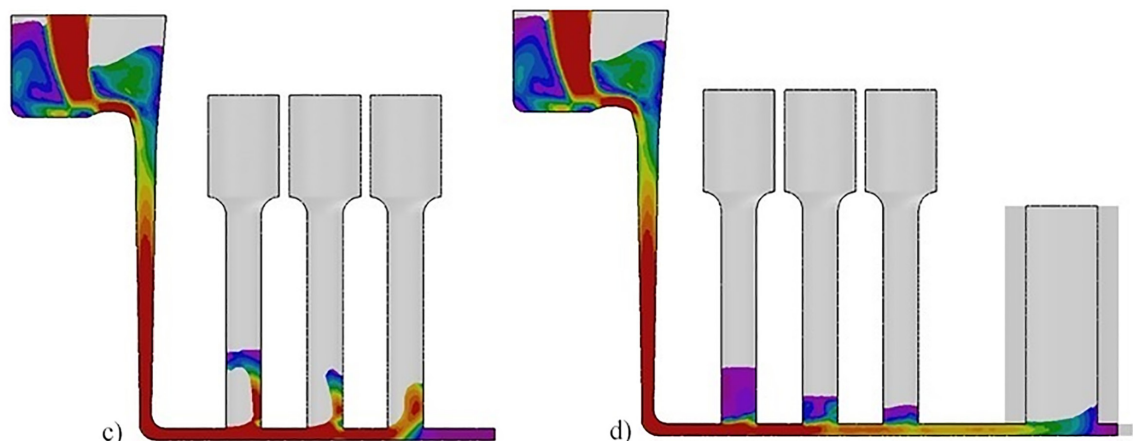

Fig. 6. Ingate velocity analysis
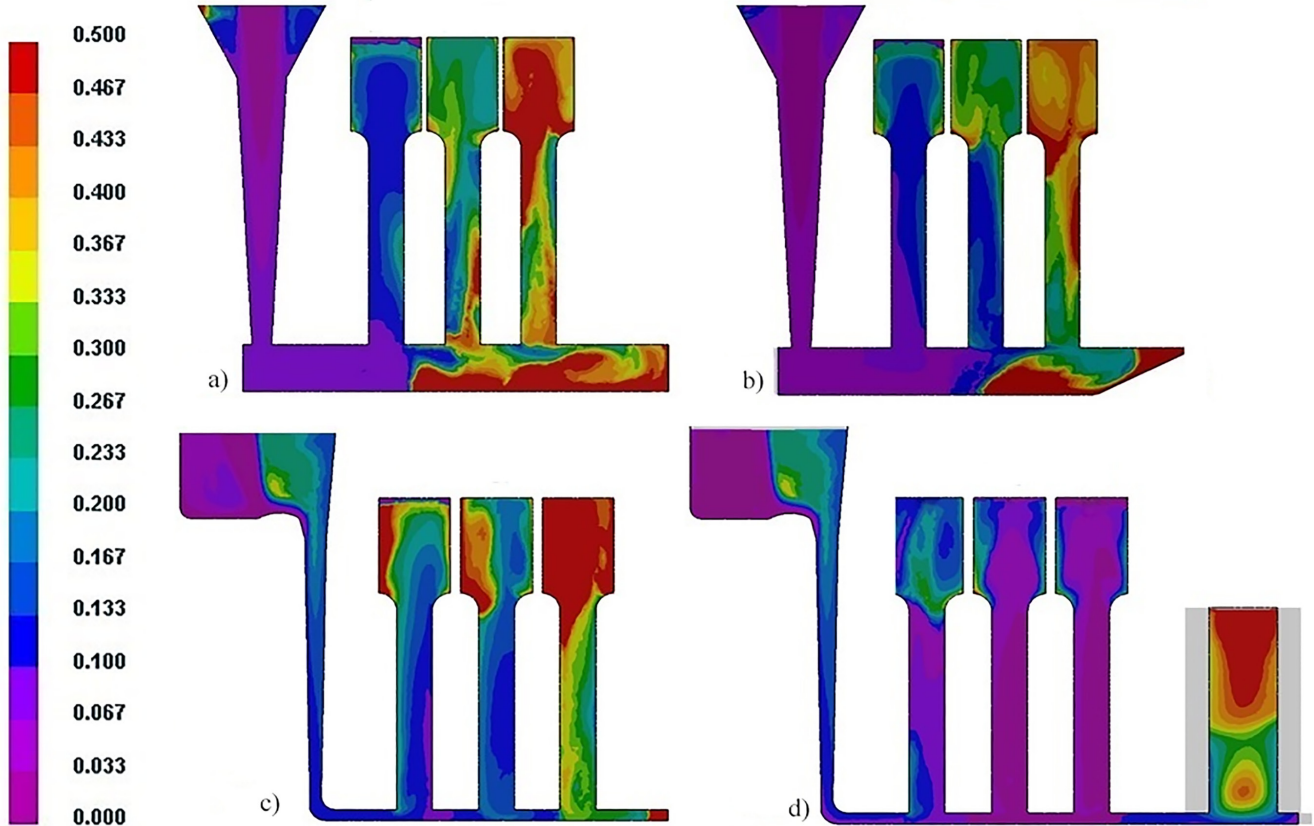
Oxides [cm²/s]

Fig. 7. Analysis of oxide occurrence

The lower values were obtained by using the naturally pressurized gating system. Based on the numerical simulation, it can be assumed that the lowest tensile strength is the result of the high content of bifilm, due to the spatter of the molten metal at the entrance to the mold cavity in the gate area.

In comparison with other types of inclusions, the presence of bifilms has a significantly more negative impact on mechanical properties, what can be attributed to the brittleness and residual gas phase contained in the interior of the bifilm. Subsequently, fracture area of samples was evaluated, examples are shown at Fig. 9.

Samples taken from gating system A shows signs of brittle fracture (fracture in one line). We can assume that it's because of the high amount of old bifilm in the sample which were created in the runner area. They are specific as brittle and weaken the functional cross-section, so we can assume that degrade
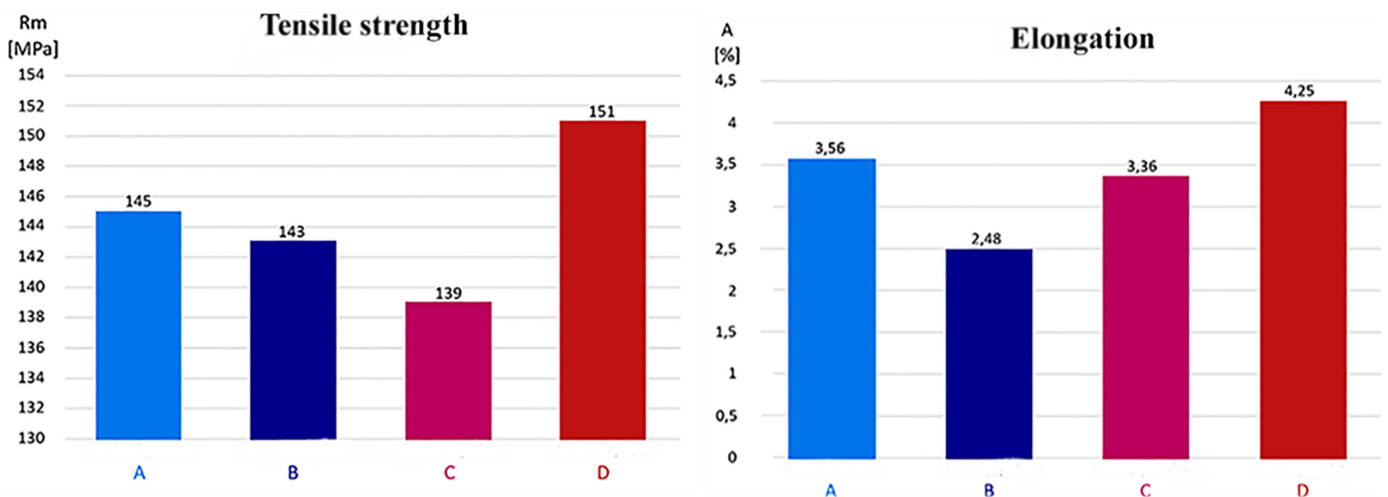

Fig. 8. Results of the tensile strength and elongation

the mechanical properties. Samples D can be specified as the ductile fracture (presence of increased amount of protrusions), caused by the presence of the young bifilms created mainly in the gate area. After evaluation of mechanical properties, the upper parts of the samples were subjected to the porosity analysis – Fig. 10.

In the Table 2 are shown arithmetical values of porosity (three samples taken for each variant from the middle cast). The worst amount of porosity was observed by naturally pressurized gating system. We can assume that it is because of extensive melt splash in the gates area. Best results was achieved by naturally pressurized system with vortex extension.
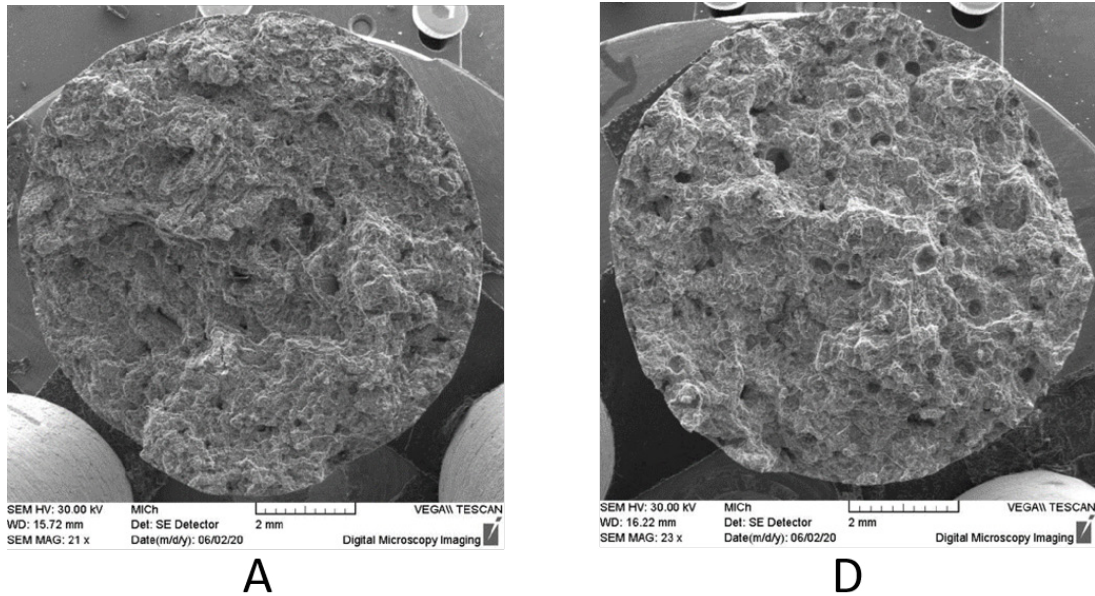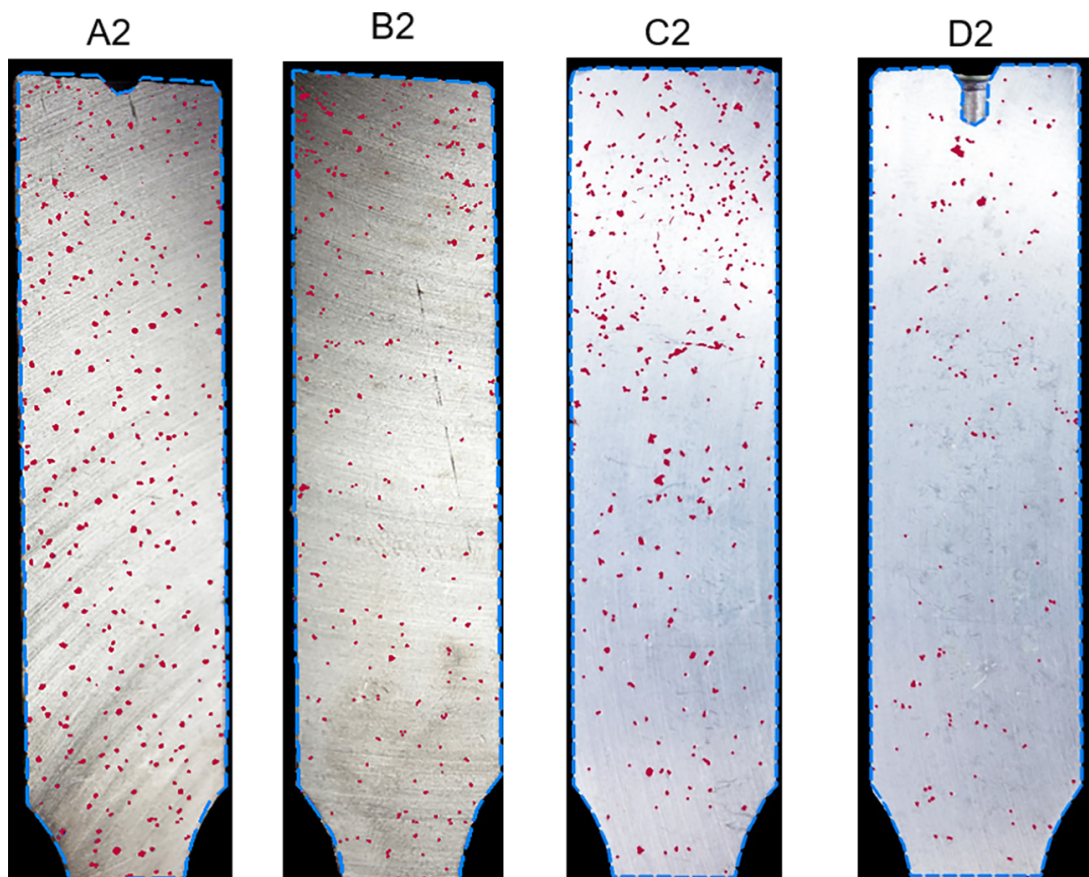

Fig. 9. Fracture area evaluation

Fig. 10. Porosity analysis

TABLE 2

Average porosity values

Gating system	A	B	C	D
Average porosity [%]	1.88	1.62	2.75	0.87

Second set of castings were used for hot tears index (HTI) evaluation. HTI criterion is determined by character and amount of tears in four arms with different length. From each alloy was casted three samples, the sample was removed from the mold after ten minutes for the visual evaluation. The HTI equation was defined according to Eq. (18).

$$HTI = \frac{NOTx\Sigma WF}{NOC} \qquad (18)$$

Where *NOT* is number of tears, *WF* is weighting factor and *NOC* is amount of casted samples. The value of the weighting factor depends on the nature and size of the individual hot tear. Fig. 11 represents coefficient values for different types of hot tears.

HTI values are shown at Table 3. In the case of non-pressurized gating system with a modification compared to a system without modification, the turbulence rate decreased by 14% (according to ProCAST). It can be seen that the *HTI* value was 0.8 lower for the naturally pressurized system then for non-pressurized gating system, this difference can be seen as a basis for further studies aimed at comparing the isolated effects of bouncing waves on the resulting rate of reoxidation processes. In the case of a naturally pressurized gating system with a vortex element applied at the end of the runner, the *HTI* rate was determined to be minimal (0.3). The vortex element ensured a smooth filling and the metal without bubbles is entering the gate.

TABLE 3

Hot tear index values

Gating system	A	B	C	D
HTI	2.25	2.1	1.3	0.3

Bifilms evaluation

For bifilms observation, SEM analysis was used. An Energy Dispersive X-Ray Analyzer (EDX) is also used to provide elemental identification and quantitative compositional information. Areas where hot tearing nucleated is with high probability a place where bifilms could occur, because of an assumption, that bifilms are the driving force for hot tearing phenomenon. The samples for metallographic observations were prepared by standard metallographic procedures (wet ground, polished with diamond pastes, finally polished with commercial fine silica slurry STRUERS OP-U) from selected hot tearing samples. The microstructure of experimental material was studied by scanning electron microscope VEGA LMU II linked to the energy dispersive X-ray spectroscopy (EDX analyzer Brucker Quantax). Fig. 12 shows the pore formed on the surface of test sample (magnification is shown directly on figure).

The observed cavities are characterized by partially irregular folds and microscopy roughness of the layer at the place of fold. Bifilm presence was confirmed mainly by a higher content of oxygen ppm % (Fig. 12). Many fragments of the oxide layer, which covered most of the pore surface may be evidence that the porosity was formed by expanse of the double oxide layer. By Papanikolau work [9], it's assumed that the presence of a relatively strong oxide layer inside a pore, could be evidence of an old bifilm from the batch material rather than a new oxide layer entrained during the filling process. The thickness of the bifilm may perhaps be an indication that the oxide had a relatively long time to absorb Mg by diffusion. Due to the low Mg content measured by EDX analysis, it can be assumed that in this case it is a relatively young bifilm entrained to the volume of melt during the filling process.

The last part of the experiment was focused on quantification of the bifilms by so called "bifilm index", which was performed based on Dispinar previous work [10]. Samples used for mechanical evaluation were remelted in IGBT vacuum furnace to minimalize the influence of new oxidization. Melt was poured into standard RPT test and consequently bifilm index was analyzed. Bifilm index represents the total length of bifilms estimated from the sectioned surface of reduced pressure test samples, using the sum of the maximum lengths of the pores "L_b" measured in millimeters, examples are shown at Fig. 13.

Three samples for gating system A and D were analyzed and average values are shown in Table 4. Achieved results can be considered as direct evidence of lower amount of bifilms in
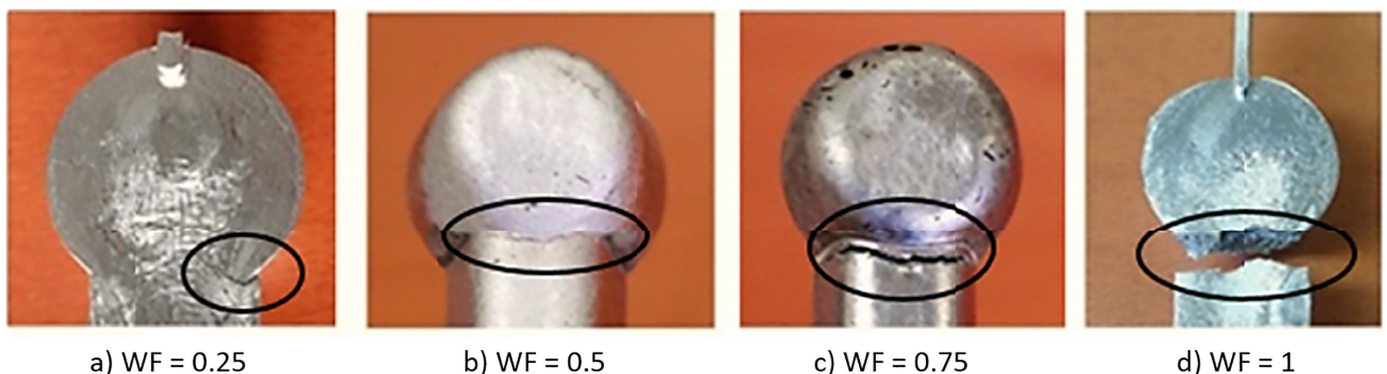

a) WF = 0.25   b) WF = 0.5   c) WF = 0.75   d) WF = 1

Fig. 11. Weighting factor values a) 0.25 b) 0.5 c) 0.75 d) 1

Image10-1						
Elt.	Intensity	Error (c/s)	Gauss 2-sig	Atomic Fit	Conc %	
O	27.45	1.913	2.43	9.063	5.573	wt.%
Mg	27.71	1.922	0.99	0.936	0.874	wt.%
Al	2 502.34	18.266	17.32	86.188	89.376	wt.%
Si	39.81	2.304	1.47	3.755	4.053	wt.%
Fe	0.96	0.358	0.22	0.058	0.124	wt.%
				100.000	100.000	wt.%
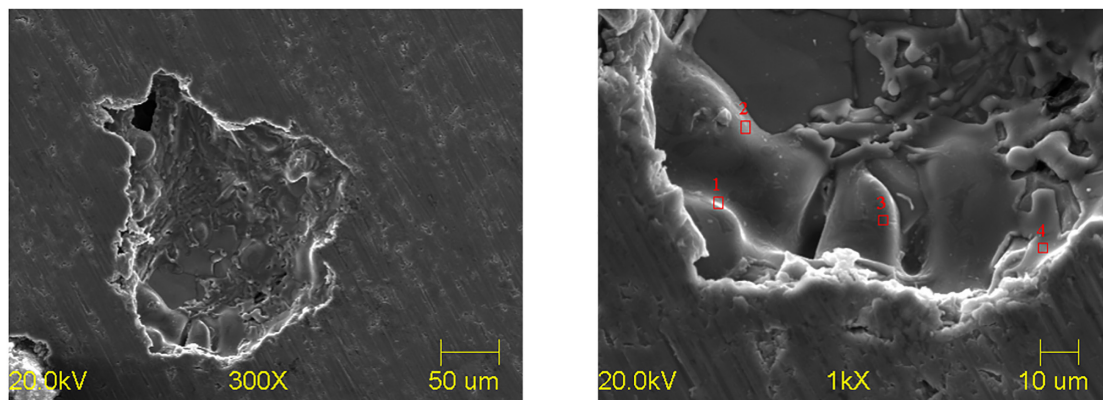
Image10-2						
Elt.	Intensity	Error (c/s)	Gauss 2-sig	Atomic Fit	Conc %	
O	21.93	1.710	2.25	7.342	4.454	wt.%
Mg	20.73	1.662	0.62	0.702	0.647	wt.%
Al	2 418.21	17.954	16.65	82.993	84.904	wt.%
Si	94.76	3.554	2.43	8.534	9.088	wt.%
Fe	7.14	0.976	0.54	0.429	0.907	wt.%
				100.000	100.000	wt.%

Image10-3						
Elt.	Intensity	Error (c/s)	Gauss 2-sig	Atomic Fit	Conc %	
O	9.09	1.101	1.19	3.419	2.055	wt.%
Mg	33.12	2.101	1.19	1.170	1.068	wt.%
Al	2 468.44	18.140	17.08	93.187	94.434	wt.%
Si	19.55	1.614	0.99	2.130	2.246	wt.%
Fe	1.40	0.431	0.24	0.094	0.197	wt.%
				100.000	100.000	wt.%

Image10-4						
Elt.	Intensity	Error (c/s)	Gauss 2-sig	Atomic Fit	Conc %	
O	19.12	1.597	3.07	7.075	4.313	wt.%
Mg	18.10	1.553	0.58	0.664	0.615	wt.%
Al	2 372.52	17.785	16.77	90.248	92.789	wt.%
Si	17.53	1.529	1.26	1.892	2.025	wt.%
Fe	1.79	0.489	0.15	0.121	0.257	wt.%
				100.000	100.000	wt.%

Fig. 12. SEM micrograph of oxide layer found at the pore on the surface of cast sample
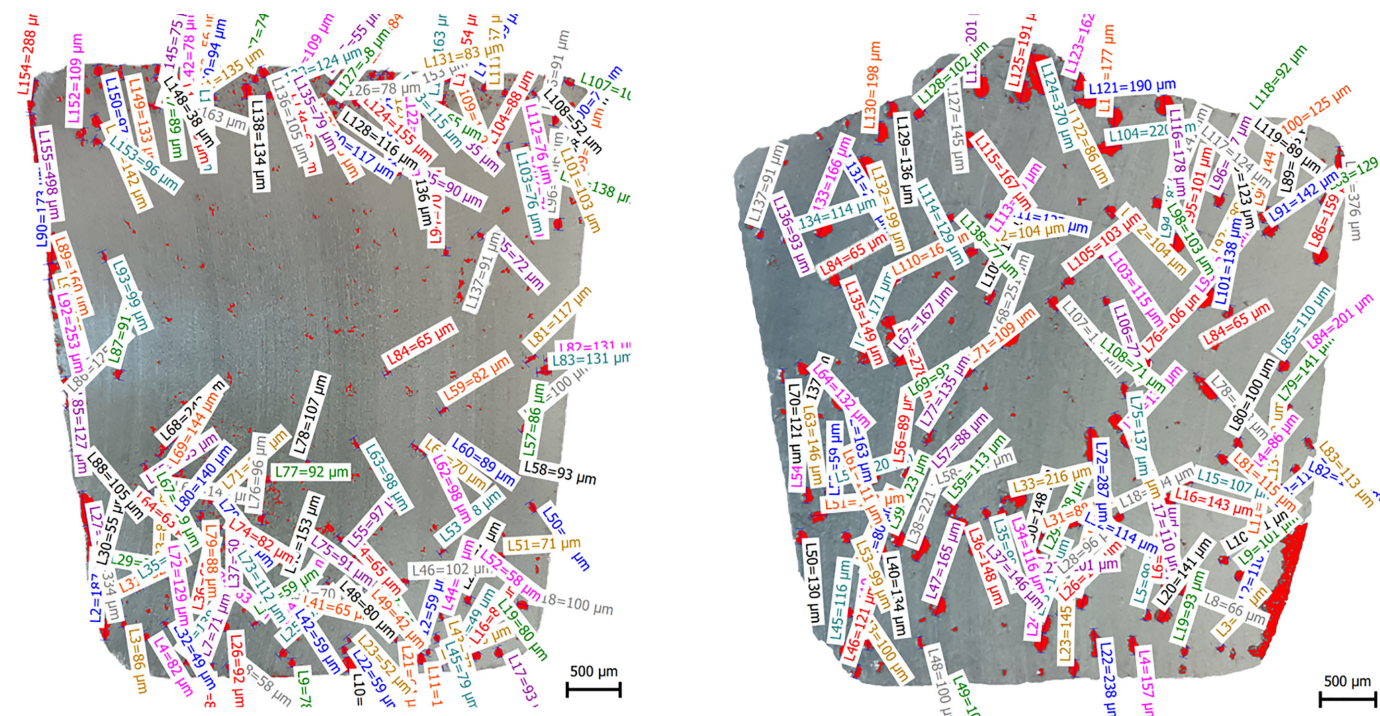

Fig. 13. Bifilm index evaluation

the gating system D, compared to gating system A, which was achieved by providing a filling system design that does not re-introduce excessive amount of bifilms to the casting.

TABLE 4

Bifilm index

Gating system	A	D
L_b [mm]	209	142

6. conclusion

– Numerical simulation proven that filling systems designed to follow the shape of the falling stream (naturally pressurized system) are successful to reduce the conditions for forming entrainment defects.

– Using of vortex element reduces the critical velocity of flow in which the melt enters the mold cavity through the gate, and also minimizes the oxide occurrence in the castings. The front head of molten metal enters the cylindrical end, where is the flow directed to a tangential gradient eddying motion.

– The mechanical properties evaluation confirmed the positive effect of the naturally pressurized gating system, but only when proper velocity reduction element is used. In case when velocity was not reduced, naturally pressurized gating system exhibited even worse tensile strength values than the common non-pressurized system.

– Hot tear index evaluation clearly confirmed the positive effect of the naturally pressurized gating system, leading to almost "hot tear free" casting in case of the naturally pressurized system with vortex element.

REFERENCES

[1] J.M. Svoboda, R.W. Monroe, C.E. Bates, J. Griffin, TAFS. **95**, 187-202 (1987).

[2] J. Campbell. Complete casting handbook 2nd edition. Oxford, Elsevier Ltd. (2015)

[3] G. Gyarmati, Gy. Fegyverneki, M. Tokár, T. Mende, Int. J. Engineering and Management Sciences **5**, 141-153 (2020). DOI: 10.21791/IJEMS.2020.2.18

[4] J. Campbell, Invisible Macrodefects in Castings, J. de Physique IV 3, 861-872 (1993). https://doi.org/10.1051/jp4:19937135

[5] M. Brůna, D. Bolibruchová, R. Pastirčák, Archives of Foundry Engineering **17**, 23-26 (2017). https://doi.org/10.1515/afe-2017-0084

[6] A. Sladek, M. Patek, M. Mician, Archives of Metallurgy and Materials **62** (3), 1597-1601 (2017), DOI: 10.1515/amm-2017-0244

[7] K. Major-Gabrys, Biodegradable materials as foundry moulding sands binders, Metalurgija **54**, 3, 591-593 (2015).

[8] J. Lago, L. Trško, M. Jambor, F. Nový, O. Bokůvka, M. Mičian, F. Pastorek, Metals **9** (6), 619 (2019), DOI: 10.3390/met9060619

[9] M. Papanikolaou, E. Pagone, M. Jolly, K. Salonitis, Numerical simulation and evaluation of Campbell running and gating systems, Metals, 10.1, art. no. **68 (**2020). DOI.org/10.3390/met10010068

[10] D. Dispinar, J. Campbell. Use of bifilm index as an assessment of liquid metal quality, International Journal of Cast Metals Research **19**, 1, 5-17 (2006). DOI: 10.1179/136404606225023300